Acta Crystallographica Section C
Crystal Structure Communications
ISSN 0108-2701

XRD and VCD: a marriage of love or convenience? Honeymoon around a cyclic urea derivative

Dragos Gherase,[a] Jean-Valère Naubron,[b] Christian Roussel[c] and Michel Giorgi[b]*

[a]C. D. Nenitzescu Center of Organic Chemistry, Romanian Academy, Spl. Independentei 202 B, 060023 Bucharest, Romania, [b]Spectropole FR1739, Aix Marseille Université, Campus de St Jérôme, Avenue Escadrille Normandie Niemen, 13397 Marseille Cedex 20, France, and [c]ISM2 UMR 7313, Aix Marseille Université, Campus de St Jérôme, Avenue Escadrille Normandie Niemen, 13397 Marseille Cedex 20, France
Correspondence e-mail: michel.giorgi@univ-amu.fr

Received 18 May 2012
Accepted 23 May 2012
Online 13 June 2012

The structures and absolute configurations of the enantiomers (3a*R*,8a*R*)-2,2-dimethyl-4,4,8,8-tetraphenyl-4,5,6,7,8,8a-hexahydro-3a*H*-1,3-dioxolo[4,5-*e*][1,3]diazepin-6-one 0.33-hydrate, $C_{32}H_{30}N_2O_3\cdot0.33H_2O$, (I*a*), and (3a*S*,8a*S*)-2,2-dimethyl-4,4,8,8-tetraphenyl-4,5,6,7,8,8a-hexahydro-3a*H*-1,3-dioxolo-[4,5-*e*][1,3]diazepin-6-one 0.39-hydrate, $C_{32}H_{30}N_2O_3\cdot0.39H_2O$, (I*b*), have been elucidated unambiguously using the complementary power of single-crystal X-ray diffraction (XRD) and vibrational circular dichroism (VCD). The enantiomers crystallize in the Sohncke space group $P2_12_12$ and pack as dimers stabilized by two symmetric hydrogen bonds involving one amide group each of the cyclic urea moiety. This double interaction is capped by a water molecule that partially occupies a site lying on the twofold axis and forms an uncommon hydrogen bond between the two monomers. A comparison between the solid-state VCD characterizations and the Bayesian statistics on Bijvoet differences determined from the XRD measurements reveals a tendency towards the correct determination of the absolute configuration by this latter method.

Comment

The determination of the absolute configuration of molecules is of crucial importance in chemistry, biology and pharmaceutics, in both industrial processes and fundamental research. Several methods can lead more or less straightforwardly to this information, but among them single-crystal X-ray diffraction (XRD) and vibrational circular dichroism (VCD) are the two methods of reference when the concern is to obtain the information directly from experimental evidence (Flack & Bernardinelli, 2008*a*; He *et al.*, 2011, and references therein). Each of these methods possesses its own advantages and drawbacks and they are now commonly coupled in studies involving absolute configuration determination. However, in most cases their association is restricted to a cross-validation process, where one method is used to confirm the results obtained by the other and *vice versa*: as in a marriage of convenience, the partners cohabit but do not interact much. The aim of this study is to show that much more structural information can be inferred from a process involving full collaboration and feedback between the two partners: a marriage for love. The starting point for the honeymoon journey was the synthesis and characterization of the (3a*R*,8a*R*) and (3a*S*,8a*S*) enantiomers of 2,2-dimethyl-4,4,8,8-tetraphenyl-4,5,6,7,8,8a-hexahydro-3a*H*-1,3-dioxolo[4,5-*e*]-[1,3]diazepin-6-one, (I), a new seven-membered ring urea derivative.

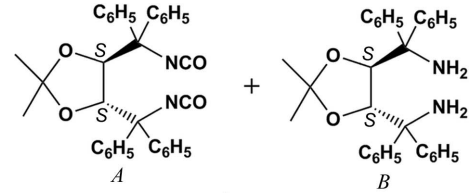

(I*a*) = (3a*R*,8a*R*)- (I)·0.33H_2O
(I*b*) = (3a*S*,8a*S*)-(I)·0.39H_2O

Cyclic urea-containing molecules are well known inhibitors of HIV-1 protease (Sussman *et al.*, 2002; Duan *et al.*, 2011, and references therein). In that context it has been proposed recently that the nature of the hydrogen-bond network between HIV-1 protease and urea-based inhibitors can be related to the efficiency of the latter (Li *et al.*, 2011).

From enantiopure tartaric acid, we synthesized the (*R*,*R*) and (*S*,*S*) enantiomers of (I), hereinafter (I*a*) and (I*b*), respectively, which were both obtained enantiopure as crystalline powders. A small amount of each sample was taken for crystallization by slow evaporation from ethanol and the remaining material was used for solid-state IR and VCD measurements.

The absolute configurations of (I*a*) and (I*b*) were known *a priori* from the synthetic process, but we decided to confirm them by solid-state VCD measurements (He *et al.*, 2011, and references therein). The solid-state IR absorption spectra of both enantiomers revealed large bands in the C=O and C—N stretching regions (1600–1750 and 1350–1500 cm^{-1}, respectively) (Fig. 1). Based on literature data and density functional

 doi:10.1107/S010827011202358X

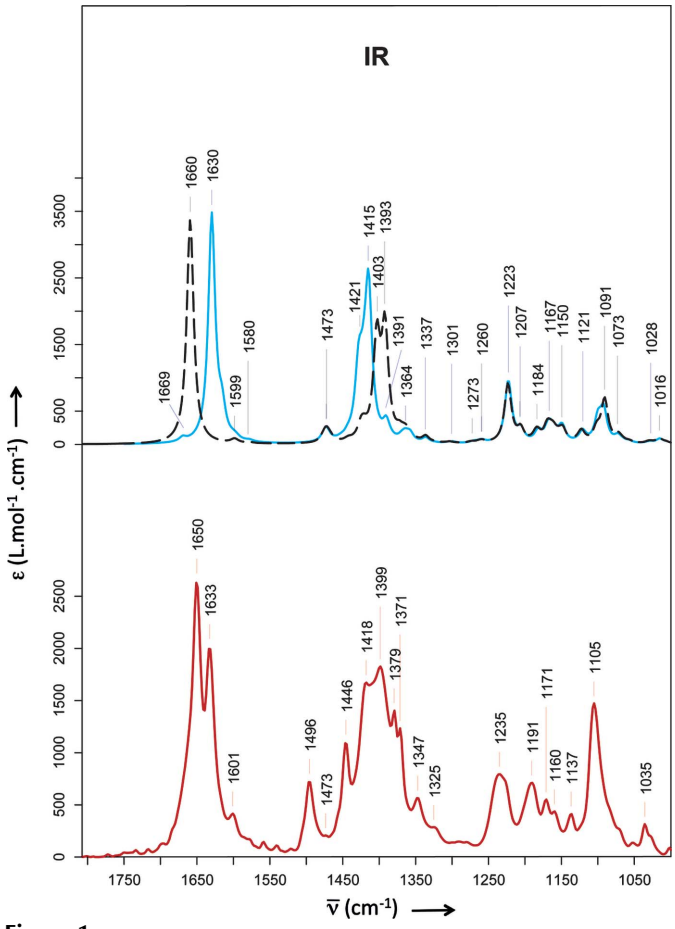

Figure 1
The solid-state IR absorption spectra for (I*a*). Lower trace: measured data (red in the electronic version of the journal). Upper traces: data calculated without water (model *A*; black dashed) or with water (model *B*; blue) at the cam-B3LYP/6-31G(d) theoretical level. A scaling factor correction of 0.94 was applied to the calculated frequencies.

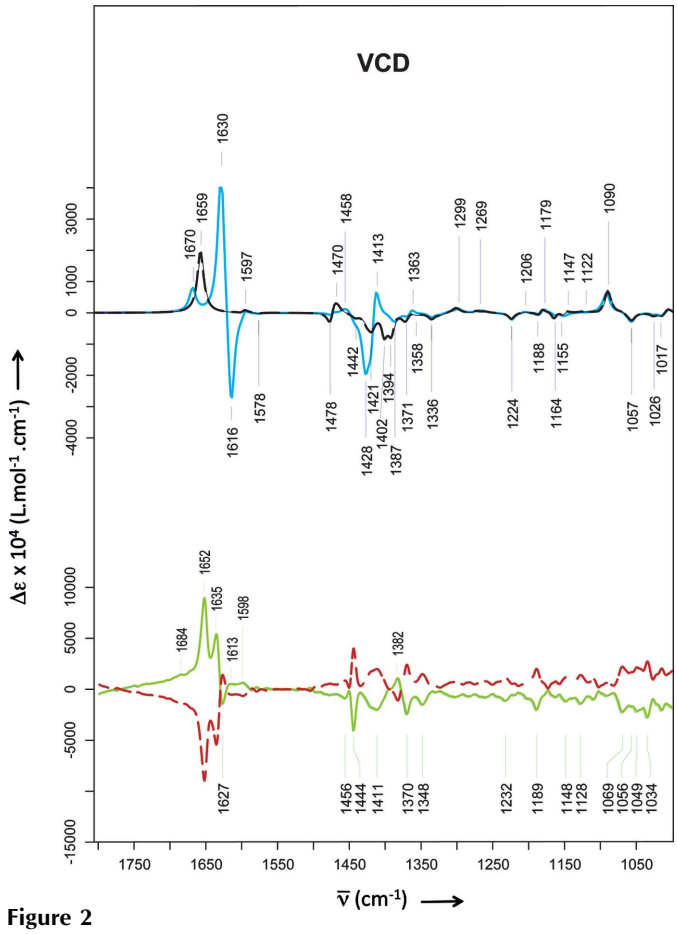

Figure 2
The solid-state VCD spectra. Lower traces: measured for (I*a*) (green in the electronic version of the journal) and (I*b*) (red dashed). Upper traces: calculated for (I*a*) without water (model *A*; black dashed) or with water (model *B*; blue) at the cam-B3LYP/6-31G(d) theoretical level. A scaling factor correction of 0.94 was applied to the calculated frequencies.

theory (DFT) calculations for interpretation of the IR spectra, it appeared that the bands at 1371, 1379 and 1650 cm^{-1} cannot be related to an isolated molecule but rather are induced by interactions between two urea moieties. However, the second $\nu_{C=O}$ band at 1633 cm^{-1}, as well as the bands at 1399, 1418, 1446 and 1496 cm^{-1}, cannot be attributed to such a supramolecular structure. It was thus necessary to determine unambiguously the solid-state structure of (I) in order to calculate the correct VCD spectra. In particular, it was essential to determine the origin of the intense positive couplet (1616 and 1630 cm^{-1}) associated with the second stretching $\nu_{C=O}$ vibrational mode (Fig. 2).

We then carried out low-temperature XRD measurements in order to determine the supramolecular structure of (I), and these data were then used as new input for the calculation of the VCD spectra. As expected from the IR spectra, (I) crystallizes as a dimer (Fig. 3). However, the asymmetric unit is composed of one molecule of (I) in a general position and a water molecule lying on a twofold axis [Figs. 4 and 5 for enantiomers (I*a*) and (I*b*), respectively]. The molecule is built around the ring including the carbamide moiety. A survey of the Cambridge Structural Database (Version 5.33; Allen, 2002) reports a few examples of ureas with this type of seven-membered ring (Czochralska *et al.*, 1977; Hodge *et al.*, 1998; Schaffner *et al.*, 2006; Aubert *et al.*, 2007; Ejsmont *et al.*, 2010). The geometric parameters within this ring in (I*a*) and (I*b*) are

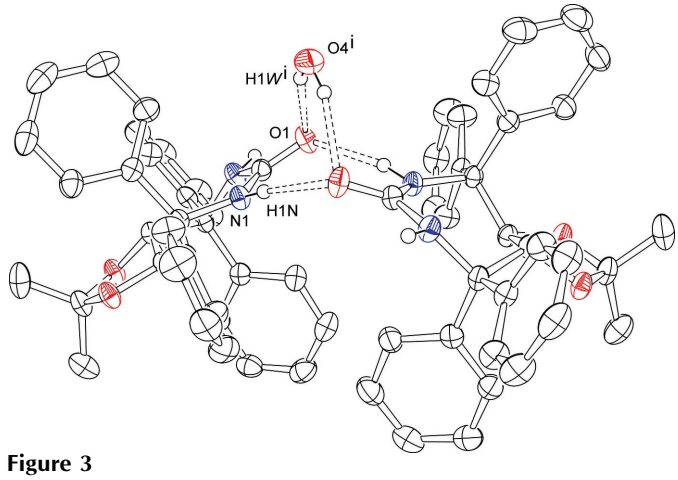

Figure 3
A representation of the dimer of (I*a*), with the hydrogen bonding to the water molecule shown with dashed bonds. Displacement ellipsoids are drawn at the 50% probability level. [Symmetry code: $-x+1, -y+1, z$.]

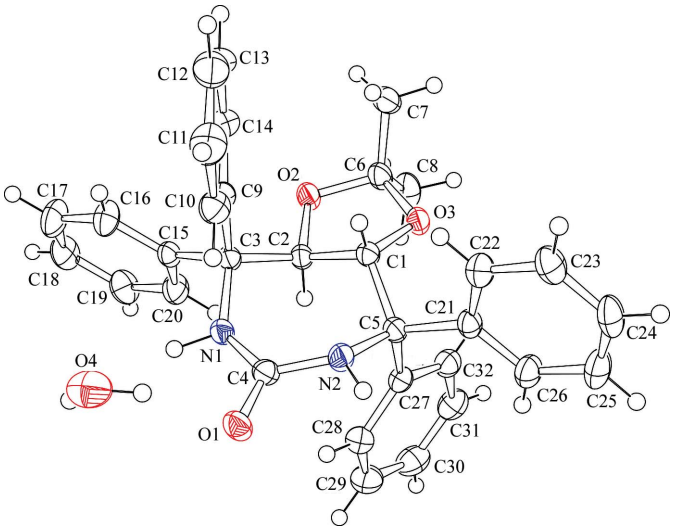

Figure 4
The molecular structure of (I*a*), showing the atom-numbering scheme. Displacement ellipsoids are drawn at the 50% probability level.

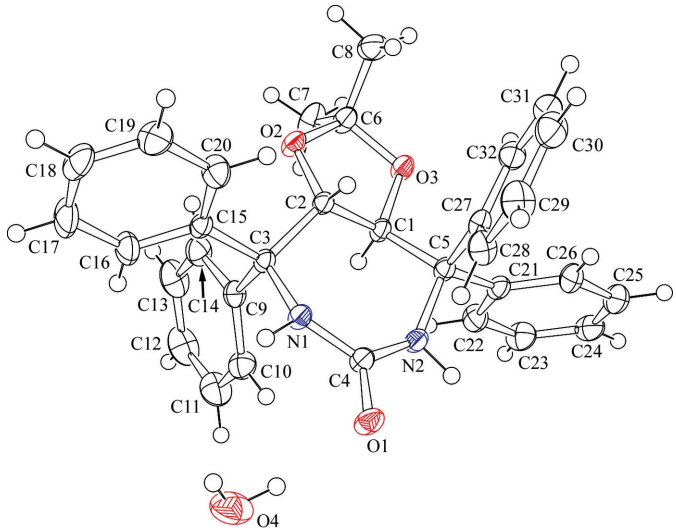

Figure 5
The molecular structure of (I*b*), showing the atom-numbering scheme. Displacement ellipsoids are drawn at the 50% probability level.

in agreement with those observed in the previously published structures, except for the angles around the N atoms of the carbamide: the C4—N1—C3 and C4—N2—C5 angles are 132.28 (16) and 131.58 (17)°, respectively, for (I*a*), and 132.08 (11) and 131.13 (11)° for (I*b*), while the values reported in the literature range from 122 to 129°. Steric hindrance due to the presence of two bulky substituents on the C atoms bonded to the N atoms can explain the opening of these angles in the present compounds. Indeed, two phenyl rings are bonded to atoms C3 and C5, and each of these pairs of rings is oriented in such a way that they are involved in intramolecular C—H$\cdots\pi$ interactions. Although the values of the characteristic geometric parameters measured in our structures are at the limit of the range commonly admitted for this kind of contact (Nishio *et al.*, 1998), it seems clear that the phenyl rings adopt conformations that tend to optimize their interaction: the H16$\cdots$C9 and H26$\cdots$C27 distances range from 2.48 to 2.49 Å, while the C16—H16$\cdots$C9 and C26—H26$\cdots$C27 angles range from 104 to 105° in the two enantiomers. Moreover, the angle defined by the two planes of each pair of interacting phenyl rings is close to 70° in all cases. This observation was confirmed by DFT calculations. Indeed, similar orientations of the pairs of phenyl rings were obtained for the optimized structure of (I), starting from the X-ray geometry and using the cam-B3LYP/6-31G(d) theoretical level (Fig. 6). The substitution of the cyclic urea is completed by the dimethyldioxolane moiety, which adopts an envelope conformation (Cremer & Pople, 1975) imposed by its connectivity to chiral atoms C1 and C2.

Interestingly, enantiomers (I*a*) and (I*b*) crystallize as dimers that interact through a double hydrogen bond between atoms O1 and N1 of two symmetry-related molecules. This double hydrogen bond is itself capped by a weaker one between a water molecule and the two O atoms of the ureas, and the network built up by these interactions resembles that of bridged cyclic hydrocarbon compounds like norbornene derivatives (Figs. 3 and 6, and Tables 1 and 2). To the best of our knowledge, this is the first example of this type of three-partner hydrogen-bond interaction involving a dimer and a water molecule.

The planes formed by the urea molecules within the dimers are neither coplanar nor twisted like those observed in three similar compounds described in the literature (Czochralska *et al.*, 1977; Ejsmont *et al.*, 2010; Aubert *et al.*, 2007). In our molecules, the angles between the two moieties are close to 53° for both (I*a*) and (I*b*), and these values are comparable with those observed in other bent geometries in similar compounds (Schaffner *et al.*, 2006) and with the simulated structures used for the VCD analysis (Fig. 6).

The weakness of the hydrogen bonds involving the water molecule is not so much a question of geometric features as of partial occupancy. On the one hand their geometric char-

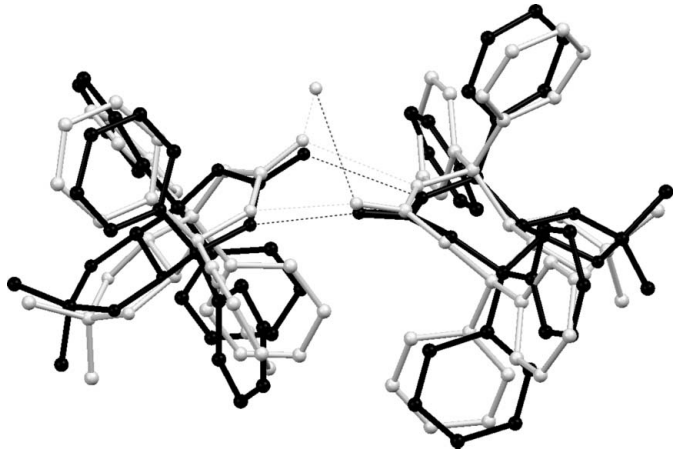

Figure 6
A superposition of the X-ray (grey) and simulated (black) structures of (I*a*). The r.m.s. deviation calculated by fitting all the non-H atoms of the five- and seven-membered rings is 0.342 Å. H atoms have been omitted for clarity. Dashed lines indicate hydrogen bonds.

acteristics are within the range of typical hydrogen bonds (Tables 1 and 2), but on the other we observed with the room-temperature XRD measurements rather high anisotropic displacement parameters for atom O4 of the water molecule, despite the stability of the crystals. We therefore supposed that this molecule was weakly bonded and labile, and on the basis of the low-temperature measurements we could refine its occupancy factor to 0.655 (9) for (I*a*) and 0.784 (8) for (I*b*) (see *Refinement*). Thus, two types of geometry co-exist in the crystalline state of (I), *viz*. a homodimeric structure, consisting of the two urea derivatives linked by a symmetric double hydrogen bond, and an uncommon heterotrimeric structure, consisting of the homodimer and a water molecule.

All these observations are in agreement with the IR and VCD measurements. The $\nu_{C=O}$ band at 1633 cm^{-1}, which was missing from the spectrum calculated without a water molecule (model *A*), was correctly modelled in the spectrum including the water molecule (model *B*) (Figs. 1 and 2). In the same way, the simulation of the spectrum of model *B* introduced two ν_{C-N} bands (1415 and 1421 cm^{-1}) which were also missing from the spectrum of model *A*. Indeed, superimposing the spectra of models *A* and *B* shows good agreement with the measured spectrum, except for two bands, 1446 and 1496 cm^{-1} (Fig. 1). These suggest a third structure which we could not assign precisely until now. However, the addition of the spectra corresponding to models *A* and *B* was sufficient to simulate the experimental VCD spectra correctly and thus to confirm the absolute configurations of (I*a*) and (I*b*) unambiguously (Fig. 2). As the samples used for VCD were derived directly from the crystalline material by crushing it under a low vacuum, a partial loss or displacement of water hydrogen bonded to the homodimer might have been induced by the mechanical constraints applied to the crystal, and one can imagine that another supramolecular structure might appear and co-exist with both the homodimer and the heterotrimer.

Stimulated by the fruitfulness of the union between XRD and VCD, we decided to extend the honeymoon a little further. The absolute configurations of both (I*a*) and (I*b*) were unambiguously determined by the VCD experiments and we were curious to know if the XRD analysis could give some indication about that information. It is often stated that the determination of absolute configuration (or absolute structure) by single-crystal XRD with an Mo *Kα* source is out of reach for compounds including only light atoms like O or N. This restriction has been generalized to enantiopure molecules for which the Friedif parameter is smaller than 80 (Flack & Bernardinelli, 2008*b*), which turns out to be the case in our study (Friedif = 5). However, it has been shown that, even if these strict requirements are not fulfilled, in many cases the absolute structure can be assigned correctly, or at least a clear indication can emerge from the data with the use of Bayesian statistics on Bijvoet differences (Hooft *et al.*, 2008). We therefore decided to test our low-temperature measurements in this way, despite the meaningless (as far as their s.u. values go) values of the refined Flack parameter. Refinements for both enantiomers were then performed by keeping the Bijvoet pairs separate (in contrast with the published refinements, where they were merged), and the results of the Bayesian statistics calculated by *PLATON* (Spek, 2009) are summarized in Table 3. Although some criteria were not optimum according to the statistics [*e.g.* the coverage of Bijvoet pairs was only 91% for (I*a*) and 95% for (I*b*), and the normal plot probability slope was less than 1], a strong tendency towards the correct assignment of the absolute configuration emerged when the refinements were performed with the correct enantiomer. This is much more clear in the case of (I*b*), where the Hooft parameter $y = 0.0$ (2) and the probabilities *P*2(true), *P*3(true) and *P*3(false) are 1.0, 0.947 and 0.0, respectively. The results obtained from the VCD measurements thus give much more confidence to these statistics than they would show in the absence of such experimental proofs. With an Mo X-ray source, more precise and complete experiments should be performed in order to enhance the anomalous signal, such as the acquisition of data with higher redundancy, or special measurements like the so-called Friedel strategy (Nonius, 1998) in order to obtain better discrimination between Bijvoet pairs. However, one can expect that further experience resulting from the accumulation of data obtained from various sources and laboratories, with coupled experiments such as XRD and VCD, will lead to increased confidence in the interpretation of Bayesian statistics and therefore to the determination of the absolute configuration of compounds of interest at the boundary of the method.

Experimental

Cyclic urea (I) was obtained by melting at 483 K a 1:1 mixture of isocyanate *A*, obtained as described by Gherase & Roussel (2012), and TADDAMINE *B*, with an overall yield of 65% after purification [see scheme for the synthesis of (I)].

Compound (I), as a well homogenized solid mixture, obtained by evaporating a solution of isocyanate *A* (258 mg, 0.5 mmol) and TADDAMINE *B* (232 mg, 0.5 mmol) in dichloromethane, was melted under argon at 483 K and kept at this temperature for 10 min. Purification by column chromatography (silica gel, diethyl ether) gave (I) (318 mg, 65%) as a colourless solid. Analysis: m.p. 528–529 K; R_F = 0.26 (1% MeOH–CH_2Cl_2); $[\alpha]_D^{25}$ = −105.5 (*c* 1.00, $CHCl_3$); ^{1}H NMR (400 MHz, $CDCl_3$): δ, 7.64–7.62 (*m*, 4H, H_{arom}), 7.40–7.38 (*m*, 6H, H_{arom}), 7.26–7.25 (*m*, 6H, H_{arom}), 7.17–7.14 (*m*, 4H, H_{arom}), 5.19 (*s*, 2H, NH), 4.56 (*s*, 2H, CH), 1.27 (*s*, 6H, CH_3); ^{13}C NMR (100 MHz, $CDCl_3$): δ 160.33 (C═S), 144.67 (C_{ipso}), 140.99 (C_{ipso}), 129.18 (CH_{arom}), 128.71 (CH_{arom}), 128.16 (CH_{arom}), 127.91 (CH_{arom}), 127.84 (CH_{arom}), 127.65 (CH_{arom}), 110.01 (C_2), 79.31 (CH), 66.09 (C_{Bz}), 27.04 (CH_3). HRMS, calculated for $C_{32}H_{30}N_2O_3$ $[M + H]^+$ 491.2329; found 491.2329. For the (3a*R*,8a*R*) enantiomer, the same procedure was employed; $[\alpha]_D^{25}$ = 105.0 (*c* 1.01, $CHCl_3$).

Suitable crystals of the (*R*,*R*) and (*S*,*S*) enantiomers were obtained by slow evaporation from ethanol.

IR and vibrational circular dichroism (VCD) spectra were recorded on a Bruker PMA 50 accessory coupled to a Vertex70 FT–IR spectrometer. A photoelastic modulator (Hinds PEM 90) set at *l*/4 retardation was used to modulate the handedness of the circular polarized light at 50 kHz. Demodulation was performed by a lock-in amplifier (SR830 DSP). An optical low-pass filter (<1800 cm^{-1}) before the photoelastic modulator was used to enhance the signal-to-

Table 1
Hydrogen-bond geometry (Å, °) for enantiomer (I*a*).

D—H···A	D—H	H···A	D···A	D—H···A
N1—H1N···O1^{i}	0.93 (2)	2.14 (2)	3.051 (2)	166.7 (12)
O4—H1W···O1^{i}	0.90	1.99	2.832 (3)	154

Symmetry code: (i) $-x+1, -y+1, z$.

Table 2
Hydrogen-bond geometry (Å, °) for enantiomer (I*b*).

D—H···A	D—H	H···A	D···A	D—H···A
N1—H1N···O1^{i}	0.897 (15)	2.198 (17)	3.0570 (16)	160.3 (11)
O4—H1W···O1^{i}	0.90	2.00	2.836 (2)	154

Symmetry code: (i) $-x+1, -y+1, z$.

noise ratio. KBr pellets were prepared by finely mixing crystals of (I*a*) or (I*b*) (1 mg) with dry purified KBr (400 mg) in an agate mortar and compressing the mixture in a mechanical press. For the individual spectrum of each enantiomer, about 1333 scans were averaged at 4 cm^{-1} resolution (corresponding to 20 min measurement time). The linear dichroism (LD) contributions to the VCD spectra were shown to be negligible from measurements of the LD spectra of the two pellets. For the IR spectra, the empty holder served as a reference. The spectra are presented without smoothing or further data processing.

All calculations were performed on enantiomer (I*a*) with absolute configuration (*R*,*R*). The geometry optimizations, vibrational frequencies, IR absorption and VCD intensities were calculated using density functional theory (DFT) with M06L and cam-B3LYP functionals combined with, respectively, 4-31G(d) and 6-31G(d) basis sets. However, only the best results, obtained at the cam-B3LYP/6-31G(d) level, are presented in this work. IR absorption and VCD spectra were constructed from calculated dipole and rotational strengths, assuming a Lorentzian band shape with a half-width at half maximum of 6 cm^{-1}. A scaling factor of 0.94 was applied to the frequencies. All calculations were performed using *GAUSSIAN09* (Frisch *et al.*, 2009).

Enantiomer (I*a*)

Crystal data

$C_{32}H_{30}N_2O_3\cdot 0.33H_20$
M_r = 496.44
Orthorhombic, $P2_12_12$
a = 14.2076 (2) Å
b = 15.9721 (3) Å
c = 11.3920 (2) Å
V = 2585.13 (8) Å^3
Z = 4
Mo $K\alpha$ radiation
μ = 0.08 mm^{-1}
T = 173 K
0.4 × 0.32 × 0.12 mm

Data collection

Nonius KappaCCD area-detector diffractometer
33303 measured reflections
6619 independent reflections
4774 reflections with $I > 2\sigma(I)$
R_{int} = 0.06

Refinement

$R[F^2 > 2\sigma(F^2)]$ = 0.053
$wR(F^2)$ = 0.147
S = 1.03
6619 reflections
344 parameters
H atoms treated by a mixture of independent and constrained refinement
$\Delta\rho_{max}$ = 0.27 e Å^{-3}
$\Delta\rho_{min}$ = −0.32 e Å^{-3}

Enantiomer (I*b*)

Crystal data

$C_{32}H_{30}N_2O_3\cdot 0.39H_2O$
M_r = 497.79
Orthorhombic, $P2_12_12$
a = 14.2212 (2) Å
b = 15.9917 (2) Å
c = 11.3920 (2) Å
V = 2590.78 (7) Å^3
Z = 4
Mo $K\alpha$ radiation
μ = 0.08 mm^{-1}
T = 173 K
0.5 × 0.4 × 0.34 mm

Data collection

Nonius KappaCCD area-detector diffractometer
44308 measured reflections
6613 independent reflections
5684 reflections with $I > 2\sigma(I)$
R_{int} = 0.041

Refinement

$R[F^2 > 2\sigma(F^2)]$ = 0.049
$wR(F^2)$ = 0.143
S = 1.14
6613 reflections
344 parameters
H atoms treated by a mixture of independent and constrained refinement
$\Delta\rho_{max}$ = 0.47 e Å^{-3}
$\Delta\rho_{min}$ = −0.52 e Å^{-3}

All H atoms were located in difference Fourier syntheses, but only the coordinates of the N-bound H atoms were refined freely, with U_{iso}(H) = 1.2U_{eq}(N). All C-bound H atoms were placed in calculated positions, with C—H = 0.93, 0.98 or 0.96 Å for aromatic, methine or methyl H atoms, respectively, and refined as rigid groups. The methyl H atoms were allowed to rotate, with U_{iso}(H) = 1.5U_{eq}(C), and for the other C-bonded H atoms U_{iso}(H) = 1.2U_{eq}(C). The position of the H atom of the water molecule was derived from a comparison between the peaks observed in the difference Fourier synthesis, the analysis of intermolecular interactions within the crystal structure and the positions of the H atoms calculated in the models for the VCD analysis. The O—H distance was fixed at 0.90 Å for both enantiomers and refined as a rigid group, with U_{iso}(H) = 1.5U_{eq}(O4).

For both (I*a*) and (I*b*), the Bijvoet pairs were merged before the final refinements. Some low-resolution reflections [six for (I*a*) and seven for (I*b*)] were found to be partially cancelled by the beam stop and were omitted from the final cycles of refinement. The occupancy factor for the water molecule in both (I*a*) and (I*b*) was refined by introducing a free variable *via* the FVAR instruction (*SHELXL97*; Sheldrick, 2008) and assigning site-occupancy factors of 21 and 22 to O and H atoms, respectively.

For both enantiomers, data collection: *COLLECT* (Nonius, 1998); cell refinement: *DENZO* and *SCALEPACK* (Otwinowski & Minor, 1997); data reduction: *DENZO* and *SCALEPACK*; program(s) used to solve structure: *SIR92* (Altomare *et al.*, 1994); program(s) used to refine structure: *SHELXL97* (Sheldrick, 2008); molecular graphics: *ORTEP-3* (Farrugia, 1997); software used to prepare material for publication: *WinGX* (Farrugia, 1999).

The authors aknowledge Dr Thierry Buffeteau, ISM, Université Bordeaux 1, for the vibrational linear dichroism (VLD) measurements and discussions. We thank the CRCMM, Aix Marseille Université, for computer time.

Table 3
Bayesian statistics on Bijvoet differences for enantiomers (I*a*) and (I*b*).

	Flack x	Hooft y	G	$P2$ (true)	$P3$ (true)	$P3$(rac-twin)	$P3$(false)
(I*a*)	−0.4 (10)	−0.4 (4)	1.80 (73)	0.999	0.918	0.081	0.1 × 10^{-3}
(I*b*)	−0.1 (7)	0.0 (2)	0.95 (39)	1.0	0.947	0.053	0.5 × 10^{-5}

Supplementary data for this paper are available from the IUCr electronic archives (Reference: SK3439). Services for accessing these data are described at the back of the journal.

References

Allen, F. H. (2002). *Acta Cryst.* B**58**, 380–388.

Altomare, A., Cascarano, G., Giacovazzo, C., Guagliardi, A., Burla, M. C., Polidori, G. & Camalli, M. (1994). *J. Appl. Cryst.* **27**, 435.

Aubert, E., Lena, G., Gellenoncourt, M., Durain, E., Guichard, G. & Didierjean, C. (2007). *Acta Cryst.* E**63**, o2306–o2308.

Cremer, D. & Pople, J. A. (1975). *J. Am. Chem. Soc.* **97**, 1354–1358.

Czochralska, B., Shugar, D., Arora, S. K., Bates, R. B. & Cutler, R. S. (1977). *J. Am. Chem. Soc.* **99**, 2583–2588.

Duan, M., Kazmierski, W. M., Tallant, M., Ho Jun, J., Edelstein, M., Ferris, R., Todd, D., Wheelan, P. & Xiong, Z. (2011). *Bioorg. Med. Chem.* **21**, 6381–6385.

Ejsmont, K., Boeglin, J., Didierjean, C., Guichard, G. & Jelsch, C. (2010). *Acta Cryst.* C**66**, o292–o294.

Farrugia, L. J. (1997). *J. Appl. Cryst.* **30**, 565.

Farrugia, L. J. (1999). *J. Appl. Cryst.* **32**, 837–838.

Flack, H. D. & Bernardinelli, G. (2008*a*). *Chirality*, **20**, 681–690.

Flack, H. D. & Bernardinelli, G. (2008*b*). *Acta Cryst.* A**64**, 484–493.

Frisch, M. J., *et al.* (2009). *GAUSSIAN09*. Gaussian Inc., Wallingford, Connecticut, USA.

Gherase, D. & Roussel, C. (2012). *Cent. Eur. J. Chem.* **10**, doi:10.2478/s11532-012-0011-8.

He, Y., Bo, W., Dukor, R. K. & Nafie, L. A. (2011). *Appl. Spectrosc.* **65**, 699–723.

Hodge, C. N., Lam, P. Y. S., Eyermann, C. J., Jadhav, P. K., Ru, Y., Fernandez, C. H., De Lucca, G. V., Chang, C.-H., Kaltenbach, R. F. III, Holler, E. R., Woerner, F., Daneker, W. F., Emmett, G., Calabrese, J. C. & Aldrich, P. E. (1998). *J. Am. Chem. Soc.* **120**, 4570–4581.

Hooft, R. W. W., Straver, L. H. & Spek, A. L. (2008). *J. Appl. Cryst.* **41**, 96–103.

Li, D., Ji, B., Hwang, K.-C. & Huang, Y. (2011). *PLoS ONE*, **6**, e19268. doi:10.1371/journal.pone.0019268.

Nishio, M., Hirota, M. & Umezawa, M. (1998). In *The C—H···π Interaction. Evidence, Nature and Consequences*. New York: Wiley-VCH.

Nonius (1998). *COLLECT*. Nonius BV, Delft, The Netherlands.

Otwinowski, Z. & Minor, W. (1997). *Methods in Enzymology*, Vol. 276, *Macromolecular Crystallography*, Part A, edited by C. W. Carter Jr & R. M. Sweet, pp. 307–326. New York: Academic Press.

Schaffner, A.-P., Lena, G., Roussel, S., Wawrezinieck, A., Aubry, A., Briand, J.-P., Didierjean, C. & Guichard, G. (2006). *Chem. Commun.* pp. 4069–4071.

Sheldrick, G. M. (2008). *Acta Cryst.* A**64**, 112–122.

Spek, A. L. (2009). *Acta Cryst.* D**65**, 148–155.

Sussman, F., Villaverde, M. C. & Martinez, L. (2002). *Protein Eng.* **15**, 707–711.